Measurement of a weak transition moment using two-pathway coherent control

D. Antypas and D. S. Elliott

Department of Physics and School of Electrical and Computer Engineering Purdue University, West Lafayette, Indiana 47907, USA

(Received 29 January 2013; published 10 April 2013)

We present a technique based upon two-pathway coherent control for the measurement of a weak transition moment. In our approach, we use two coherent optical beams, one the second harmonic of the other, to drive a transition by means of three distinct optical interactions. The interference between these interactions allows a determination of one moment relative to another. In this work, we demonstrate the approach by applying it to an experimental determination of the magnetic dipole moment for the $6s\ ^2S_{1/2} \rightarrow 7s\ ^2S_{1/2}$ transition in atomic cesium. Our results are in excellent agreement with previous single-beam measurements. We also discuss prospects for extending this measurement technique to a new determination of the weak-force induced parity-nonconserving moment on this same transition.

DOI: 10.1103/PhysRevA.87.042505 PACS number(s): 32.70.Cs, 32.80.Qk

The exchange of the weak neutral Z^0 boson between the nucleons and electrons in atomic systems can induce a very weak parity nonconserving (PNC) transition moment between atomic eigenstates [1,2]. Precise measurements of these moments can then provide a sensitive means of investigating the weak force at low momentum exchanges. Atomic cesium has played a central role in these measurements [3–6], including the most precise measurement of the weak-charge-induced transition moment $\mathcal{E}_{\rm PNC}$ [6]. PNC moments have also been measured in thallium [7–10], ytterbium [11,12], lead [13,14], and bismuth [15], and several groups are actively pursuing PNC measurements in various atomic systems. To date, however, the precision of neither the measurements nor of the atomic structure calculations in any of these other systems have reached the level of those of cesium.

Motivated by the need to resolve long-standing questions regarding the large nuclear spin dependence of $\mathcal{E}_{\rm PNC}$ reported in Ref. [6], and also by recent improvements of the atomic structure calculations in cesium [16–18], we have recently begun development of a technique, based upon two-pathway coherent control, for the measurement of extremely weak optical transitions in atomic systems. In the present study, we demonstrate this technique with a new determination of the magnetic dipole moment of the $6s\ ^2S_{1/2} \rightarrow 7s\ ^2S_{1/2}$ transition in cesium.

We previously observed [19,20] an interference between two-photon absorption and a Stark-induced transition on the $6s\ ^2S_{1/2} \rightarrow 8s\ ^2S_{1/2}$ transition in cesium. We now show how this interference can be used to measure the ratio of one weak moment relative to another. We note that most previous determinations of weak transition moments also use the interference between the weak transition and a much stronger interaction on the same transition. Our technique differs, however, in that we apply not one, but two, coherent laser fields to the atoms. The first field component $\boldsymbol{\varepsilon}^{\omega_1}$, at a wavelength of $\lambda = 540$ nm, is resonant with the transition directly, and drives the interaction through linear interactions (magnetic dipole and Stark-induced electric dipole). A critical requirement for the measurement technique is that the amplitudes for these linear interactions differ in phase by $\pi/2$, causing these two terms to add in quadrature. The second field component $\boldsymbol{\varepsilon}^{\omega_2}$, whose frequency is half that of the first, at a wavelength $\lambda = 1079$ nm, drives the same atomic transition by way of a two-photon interaction ($2P$). This additional laser field presents us with several advantages over previous techniques: (1) The continuous control of the phase difference between the strong two-photon amplitude and the various weaker transition amplitudes provides us our primary means of reversing the interference; so (2) precise reversal of large dc fields is not necessary; and (3) we employ linearly polarized laser fields.

The total transition rate W for the excitation of the $6s\ ^2S_{1/2},F,m \rightarrow 7s\ ^2S_{1/2},F',m'$ transition is proportional to the square of the sum of the amplitudes for the transition

$$W \propto |A_{2P} + A_{St} + A_{M_1}|^2, \tag{1}$$

where the terms A represent the transition amplitudes for the various interactions. F, m, F', and m' represent the total angular momentum, including nuclear spin, and its projection onto the z axis, of the ground $6s$ state, and the excited $7s$ state, respectively. These amplitudes depend on the polarization of the optical fields and the orientation of the static electric and magnetic fields $\mathbf{E} = E_y\,\hat{\mathbf{y}}$ and $\mathbf{B} = B_z\,\hat{\mathbf{z}}$ that we apply to the atoms. We follow the notation of Gilbert and Wieman [21] for explicit forms of these moments, and select the specific experimental geometry that allows us to measure M_1. For $\Delta m = 0$ transitions, the transition amplitude of the Stark-induced transition amplitude is

$$A_{St} = \left[\alpha \mathbf{E}\cdot\boldsymbol{\varepsilon}^{\omega_1}\delta_{F,F'} + i\beta(\mathbf{E}\times\boldsymbol{\varepsilon}^{\omega_1})_z C_{F,m}^{F',m}\right] e^{i\phi^{\omega_1}}, \tag{2}$$

the magnetic dipole amplitude is

$$A_{M_1} = (\hat{\mathbf{k}}\times\boldsymbol{\varepsilon}^{\omega_1})_z M_1 C_{F,m}^{F',m}\, e^{i\phi^{\omega_1}}, \tag{3}$$

and the two-photon interaction driven by the 1079-nm laser beam is

$$A_{2P} = \tilde{\alpha}\,(\varepsilon^{\omega_2}\, e^{i\phi^{\omega_2}})^2. \tag{4}$$

In these expressions, α and β are the scalar and vector polarizabilities, which characterize the transition amplitude induced by $\mathbf{E}$ when this static field is parallel to (α) or perpendicular to (β) the laser polarization $\boldsymbol{\varepsilon}^{\omega_1}$. The polarizabilities α and β are each purely real parameters. For this transition, the most precise determination of the scalar polarizability

is $\alpha = -269.7\,(11)\,a_0^3$ [22], and for the vector polarizability $\beta = 26.99\,(5)\,a_0^3$ [22–26], where a_0 is the Bohr radius, and the number in parentheses is the uncertainty. The terms $C_{F,m}^{F',m'}$ are related to the Clebsch-Gordon coefficients, and are tabulated for this transition in Ref. [21]. Ordinarily, one can disregard the optical phases ϕ^{ω_1} and ϕ^{ω_2} of the laser fields, but we must retain these terms here to properly determine the interference between the linear amplitudes and the two-photon transition amplitude. M_1 is the magnetic dipole transition moment. To first order, this transition is magnetic-dipole forbidden, but mixing due to configuration interactions and relativistic effects relaxes this restriction [27,28].

The two-photon moment $\tilde{\alpha}$ has a form similar to that of the scalar polarizability α, except the energy denominator differs to reflect the detuning of the laser frequency from single-photon resonances with intermediate states [2]. Since the two photons are of a single frequency in our measurements, $\omega_2 = \omega_1/2$, and the two-photon process can excite only $\Delta F = 0$, $\Delta m = 0$ transitions [29–31]. This feature allows us to ignore $\Delta m = \pm 1$ transitions via the M_1 or Stark-induced moments, which greatly simplifies our experimental determination.

Without loss of generality, we define the y direction to be aligned with $\hat{\mathbf{k}}$, the propagation direction of the 540-nm beam, such that the y component of the electric field $\boldsymbol{\varepsilon}^{\omega_1}$ associated with this beam must vanish for a plane wave or a weakly focused beam. This beam is linearly polarized primarily along the x axis. With the laser frequency tuned to the $\Delta F = 0$ transition, the sum of the transition amplitudes is

$$\sum A = A_{2P} + \alpha\left(E_x\varepsilon_x^{\omega_1} + E_z\varepsilon_z^{\omega_1}\right)e^{i\phi^{\omega_1}} - \{i\beta E_y + M_1\}\varepsilon_x^{\omega_1}e^{i\phi^{\omega_1}}C_{F,m}^{F,m}, \quad (5)$$

where $C_{4,m}^{4,m} = -C_{3,m}^{3,m} = m/4$ [21]. The primary terms in this expression are the dominant two-photon term A_{2P}, the Stark term $i\beta E_y\,\varepsilon_x^{\omega_1}$, and the magnetic dipole term $M_1\,\varepsilon_x^{\omega_1}$. The latter two terms differ in phase by $\pi/2$. From our measurements, described later, we estimate that $A_{2P} \approx 10^4\,A_{M_1}$, while A_{St} varies from 0 to $\sim 3\,A_{M_1}$. The two terms proportional to the scalar polarizability α are small for our experimental geometry. We will retain the $\alpha E_x\varepsilon_x^{\omega_1}$ term to properly account for the misalignment of the fields. As we vary the optical phase difference $\Delta\phi \equiv 2\phi^{\omega_2} - \phi^{\omega_1}$, the excitation rate W modulates sinusoidally, with the signal proportional to

$$W \propto \left|\sum A\right|^2 \approx |A_{2P}|^2 - K(E_y)\cos\{\Delta\phi - \delta\phi(E_y)\}, \quad (6)$$

where we have omitted the negligibly small term that is second order in $\varepsilon_x^{\omega_1}$. This signal consists of a nonvarying term due to the two-photon interaction alone, and a modulating term resulting from the interference between the two-photon amplitude and the weaker Stark-induced and magnetic-dipole amplitudes. The amplitude of the modulation is

$$K(E_y) = 2\,|A_{2P}|\,\varepsilon_x^{\omega_1}\,C_{F,m}^{F,m}\,\eta \times \sqrt{\left(M_1 - \alpha E_x/C_{F,m}^{F,m}\right)^2 + (\beta E_y)^2}, \quad (7)$$

where η, whose maximum value is 1, accounts for the spatial overlap and alignment between the ω_1 and ω_2 beams [19,20].

The phase $\delta\phi(E_y)$ is

$$\delta\phi(E_y) = \tan^{-1}\left[\beta E_y\big/\left(M_1 - \alpha E_x\big/C_{F,m}^{F,m}\right)\right]. \quad (8)$$

The amplitude $K(E_y)$ is minimized when $E_y \approx 0$, and grows with increasing $|E_y|$ as a hyperbolic function.

Our measurement of M_1, then, is carried out by applying a static field E_y to the atoms and measuring the amplitude $K(E_y)$ and phase $\delta\phi(E_y)$ of the modulation of the signal as we vary the optical phase difference $\Delta\phi$. Note that, while the two-photon process is integral to the interference, the measurement of the amplitude of the modulation versus E_y provides a direct determination of M_1/β, and is insensitive to the two-photon amplitude. Careful matching of the wavefronts of the two optical beams helps produce the largest amplitude of the modulation signal (i.e., $\eta \to 1$), but a perfect match is not required, nor is a calibration of the two-photon transition rate. This feature is critical to the measurements.

We carry out the measurements in an effusive beam of Cs atoms, housed inside a vacuum chamber evacuated to a pressure of $\sim 2.5 \times 10^{-6}$ torr. We have constructed the Cs beam nozzle using an array of stainless steel capillary tubes [32], producing a high-density, collimated beam of atoms of height 3 mm by width 1 cm. The atomic beam is crossed by laser beams in three regions, as we show in Fig. 1. We label these regions the "preparation" region, the "interaction" region, and the "detection" region, respectively. In the preparation region, the atoms are optically pumped into a specific sublevel of the ground state using a pair of external cavity diode lasers (ECDL) tuned to the Cs $6s\,^2S_{1/2} \to 6p\,^2P_{3/2}$ level at 852 nm. We control the polarization of these beams to drive the ground-state population of the atomic beam to a single magnetic component. By selecting the frequency and polarization we can choose any one of the four "extreme" components of the ground state (the $m = \pm F$ component of the $F = 3$ or $F = 4$ hyperfine level) as the initial atomic state for our measurements of M_1/β. In this region, we apply a dc magnetic field of magnitude $B \sim 2$ G in the direction of the laser propagation $\hat{\mathbf{k}}$. We have determined that, at the high atomic beam densities (estimated at $\sim 5 \times 10^9$ cm^{-3}) used for these measurements, $\sim 92\%$ of the atoms are transferred to this initial state. This preparation scheme is similar to that discussed by Wood [33].

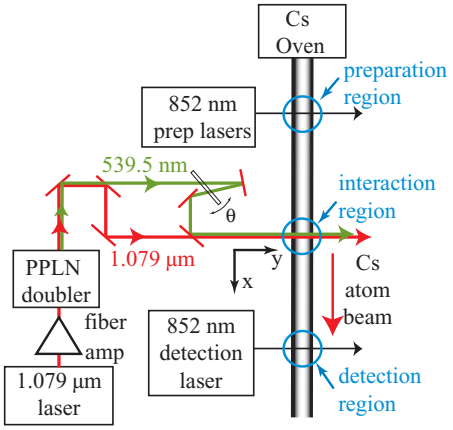

FIG. 1. (Color online) A schematic layout of the measurement system.

After the atoms are prepared in the ground state, they travel to the interaction region of the atomic beam, where they are driven by the two-frequency (ω_1 and $\omega_2 = \omega_1/2$) laser beam. We generate this beam using a homemade Littrow-style ECDL operating at $\lambda = 1079$ nm, producing an optical power of about 50 mW. We stabilize this laser frequency to the $6s \rightarrow 7s$ two-photon absorption line in a Cs vapor cell, and amplify this 1079-nm beam using a commercial fiber amplifier system to a power of 12 W. Using a magnesium-doped periodically poled lithium niobate (MgO:PPLN) crystal, we frequency double a portion of this beam, producing more than 800 mW of light at 539.5 nm. This second harmonic beam is coherent to and propagating colinear with the 1079-nm beam. We separate the two components, phase delay the green beam, and recombine the beams before directing them toward the interaction region of the atom beam inside the vacuum chamber. We delay the phase of the green beam using a rotating optical flat mounted on a galvanometer. We double pass the green beam through this optical flat to minimize beam displacement. We apply a linear ramp voltage (∼0.1 Hz) to the galvanometer, sweeping the galvanometer angle θ, producing a slow, nearly linear variation of the relative optical phase, which we label $\Delta\phi_{\rm scan}$. In addition, we apply a higher frequency (∼150 Hz) dither signal to the galvanometer, producing a sinusoidal modulation of the phase $\Delta\phi_{\rm mod}$. The sum of these phases $\Delta\phi = \Delta\phi_{\rm scan} + \Delta\phi_{\rm mod}$ gives rise to a modulation in the excitation rate of the $7s$ state of the cesium atoms, as given by Eq. (6).

We apply a 7-G magnetic field in the z direction (vertical) to the atoms in the interaction region, and a variable electric field in the y direction. We generate the electric field by applying a potential difference V between a pair of parallel aluminum plates of dimension 15 × 15 cm, separated by a spacing of $d = 5.338\,(7)$ cm and coated with a thin layer of Aquadag. A 2.5-mm diameter hole in the center of each plate admits the interaction laser beams. Through numerical modeling of the electric field, we have determined that the variation of this field over the interaction volume is less than 0.05%.

After excitation by the interaction beams, the atoms travel downstream to the detection region, where they are intersected by a laser beam tuned to 852 nm. This laser drives the $6s\ ^2S_{1/2} \rightarrow 6p\ ^2P_{3/2}$ cycling transition, and we detect the fluorescence scattered by atoms in a scheme patterned after that developed by the Boulder group [33]. We tune the frequency of the detection laser to be resonant with the hyperfine line from the component of the ground state that was initially emptied by the preparation beam. Atoms that were excited to the $7s$ state in the interaction region relax spontaneously to the ground state, with a significant probability (of order 1/2) of landing in the hyperfine component that was emptied by the preparation laser. We detect the fluorescent light scattered by these atoms as they are driven by the detection laser, with about ten photons detected per atom passing through this region, using a large area photodiode placed close to the atom beam. An interference filter reduces the light levels arising from other sources, and we amplify the photocurrent in a pre-amplifier. We measure the component of the $7s$ excitation rate modulating at 150 Hz (the dither frequency applied to the galvo plate) as a function of E_y using a lock-in amplifier for phase-sensitive detection. We compute the amplitude of the peak of the Fourier transform of these data to determine the amplitude $K(E_y)$. To reduce the effect of slight drifts in the signal (resulting from variations in the overlap of the 1079- and 540-nm beams, the power of the 540- and 1079-nm laser beams, and the density of the Cs beam), we alternate measurements of the signal with field E_y applied and zero field. We repeat this at several different values of E_y, and show a plot of $K(E_y)/K(0)$ in Fig. 2. The cesium atoms are prepared in the $F = 3, m = -3$ state for these data. We show three data points at each field value E_y, with each data point representing the average of five measurements of $K(E_y)/K(0)$. Only ∼80 s were required to acquire each data point. For the data shown, the least-squares fit to Eq. (7) yields the value $|M_1/\beta| = 29.80\,(29)$ V/cm. The only other adjustable parameter in this fit is the small angle between $\mathbf{E}$ and the propagation direction $\hat{\mathbf{k}}$. We carry out each measurement four times under the same initial conditions, and repeat the procedure discussed above after preparation of the initial ground state in each of four different cases (i.e., $F = 3$ or 4, with $m = \pm F$). We illustrate the individual results of the 16 determinations of $|M_1/\beta|$ in Fig. 3. From the variation of the phase $\delta\phi(E_y)$ as a function of E_y, not shown, we determine that the value of M_1/β is negative.

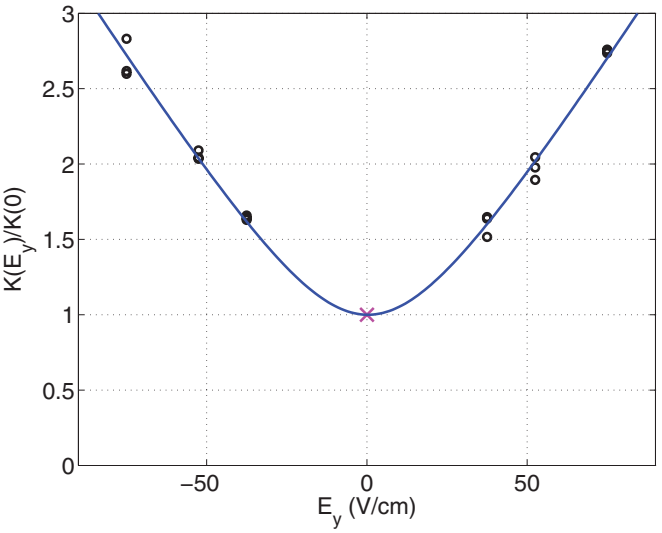

FIG. 2. (Color online) The normalized amplitude $K(E_y)/K(0)$ as a function of E_y. The data points represent our measurements. The solid line represents a fit of Eq. (7) to the data.

The primary sources of uncertainty in these measurements are due to amplitude and frequency fluctuations of the 852-nm detection laser (15 ppm/$\sqrt{\rm Hz}$), shot noise in the excitation process (10 ppm/$\sqrt{\rm Hz}$), power noise in the excitation laser (8 ppm/$\sqrt{\rm Hz}$), and shot noise related to the residual population in the initially "empty" ground state (5 ppm/$\sqrt{\rm Hz}$). The effect of pointing instabilities in the interaction beam is difficult to quantify, but they appear to be well accounted for in our method of data collection. The combined noise density of ∼25 ppm/$\sqrt{\rm Hz}$ corresponds to a signal-to-noise ratio of about 3 in 1 s of integration time. This roughly agrees with our quoted 0.3% uncertainty in M_1/β after about 2×10^4 s of data collection time. In addition, we estimate the following systematic uncertainties in our determination of the electric field produced by the parallel field plates: 0.14% from the field plate spacing, 0.034% for the uncertainty

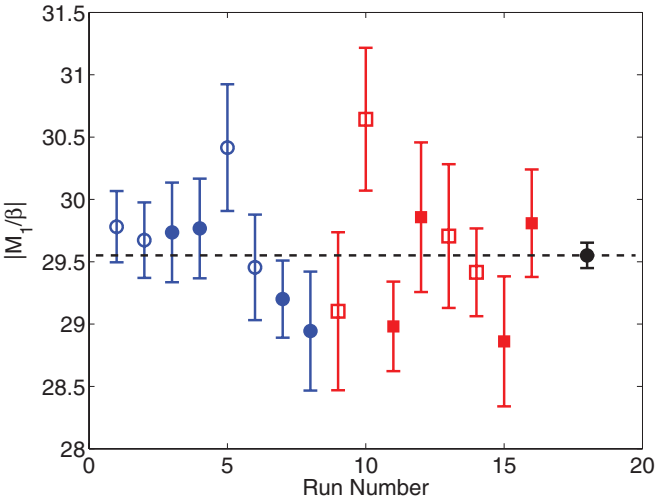

FIG. 3. (Color online) Results of the 16 individual determinations of M_1/β. The (blue) circles represent $|M_1/\beta|$ for initial states in the $F = 3$ hyperfine line, while (red) squares are for the initial $F = 4$ hyperfine line. We use open symbols for results from $m = -F$ initial states and closed symbols for results from $m = +F$ initial states. The dashed line and black solid round data point at the right represent the weighted average of the individual results.

in the voltage measurement, and 0.07% due to instrumental variations between channels of the data acquisition system.

Our final determination of M_1/β is $-29.55\,(10)_{\text{stat}}(5)_{\text{sys}}$ V/cm, where we give the statistical and systematic uncertainties individually. This is consistent with the previously measured values by Gilbert, Watts, and Wieman [34] of $M_1/\beta = -29.73\,(34)$ V/cm; $M_1/\beta = -29.55\,(45)$ V/cm by Bouchiat, Guéna, and Pottier [35]; and $M_1/\beta = -29.48\,(7)$ V/cm by Bennett [36]. Using $\beta = 26.99\,(5)\,a_0^3$ [22–26], our measurement result for M_1 is $-4.251\,(18) \times 10^{-5}\,|\mu_B|/c$, where $\mu_B = \frac{e\hbar}{2m_e c}$ is the Bohr magneton. Agreement with the latest theoretical result [28] $M_1 = -3.58 \times 10^{-5}\,|\mu_B|/c$ is reasonable, considering the difficulty of calculating this moment.

As we stated previously, our long-term goal is an application of this technique to a measurement of the weak-force-induced interaction on the same transition, with essentially the same apparatus. The field configuration for such a measurement must be altered, with **E**, **B**, and $\boldsymbol{\varepsilon}^{\omega_1}$ each aligned with the z axis. Since the magnitude of $\mathcal{E}_{\text{PNC}}$ is smaller than that of M_1, by a factor of $\sim 2 \times 10^4$, several improvements to our apparatus will be required. An optical power build-up cavity to enhance the amplitude $\boldsymbol{\varepsilon}^{\omega_1}$ will be necessary. Such a cavity is also used in other measurements of the PNC amplitude [6,11,12]. With a Finesse of 10^4, we can enhance the field amplitude by $\sim 10^2$. In contrast to techniques used elsewhere in which the cavity supports a standing wave mode, we must use a traveling-wave configuration to maintain the interference phase across the interaction region. This optical cavity can also be used to improve the polarization purity of $\boldsymbol{\varepsilon}^{\omega_1}$ [37], which will be necessary to reduce the systematic effects due to the magnetic dipole amplitude. Further suppression of the noise on the frequency of the 1079-nm laser and the detection laser will be necessary for this measurement, as will longer integration times. With each of these improvements in place, the application of the two-pathway coherent control scheme to measurement of the PNC interaction, while challenging, should be attainable.

We have reported a technique based upon coherent control ideas for the measurement of weak optical interaction moments. Our measurement of M_1 is in good agreement with previous measurements. We are extending this technique for application toward the weak-force-induced amplitude $\mathcal{E}_{\text{PNC}}$.

We are happy to acknowledge the support of the National Science Foundation under Grant No. PHY-0970041 of this work. Helpful discussions with M. S. Safronova, C. Tanner, and C. Weiman, and contributions by T. Miller, A. Altaf, S. Dutta, R. Ding, and A. Loveless are also acknowledged.

[1] M. A. Bouchiat and C. Bouchiat, J. Phys. **35**, 899 (1974).
[2] M. A. Bouchiat and C. Bouchiat, J. Phys. **36**, 493 (1975).
[3] M. A. Bouchiat, J. Guéna, L. Hunter, and L. Pottier, Phys. Lett. B **117**, 358 (1982).
[4] S. L. Gilbert, M. C. Noecker, R. N. Watts, and C. E. Wieman, Phys. Rev. Lett. **55**, 2680 (1985).
[5] J. Guéna, M. Lintz, and M. A. Bouchiat, Phys. Rev. A **71**, 042108 (2005).
[6] C. S. Wood, S. C. Bennett, D. Cho, B. P. Masterson, J. L. Roberts, C. E. Tanner, and C. E. Wieman, Science **275**, 1759 (1997).
[7] P. H. Bucksbaum, E. D. Commins, and L. R. Hunter, Phys. Rev. D **24**, 1134 (1981).
[8] P. S. Drell and E. D. Commins, Phys. Rev. A **32**, 2196 (1985).
[9] N. H. Edwards, S. J. Phipp, P. E. G. Baird, and S. Nakayama, Phys. Rev. Lett. **74**, 2654 (1995).
[10] P. A. Vetter, D. M. Meekhof, P. K. Majumder, S. K. Lamoreaux, and E. N. Fortson, Phys. Rev. Lett. **74**, 2658 (1995).
[11] K. Tsigutkin, D. Dounas-Frazer, A. Family, J. E. Stalnaker, V. V. Yashchuk, and D. Budker, Phys. Rev. Lett. **103**, 071601 (2009).
[12] K. Tsigutkin, D. Dounas-Frazer, A. Family, J. E. Stalnaker, V. V. Yashchuk, and D. Budker, Phys. Rev. A **81**, 032114 (2010).
[13] D. M. Meekhof, P. A. Vetter, P. K. Majumder, S. K. Lamoreaux, and E. N. Fortson, Phys. Rev. A **52**, 1895 (1995).
[14] S. J. Phipp, N. H. Edwards, P. E. G. Baird, and S. Nakayama, J. Phys. B **29**, 1861 (1996).
[15] M. J. D. Macpherson, K. P. Zetie, R. B. Warrington, D. N. Stacey, and J. P. Hoare, Phys. Rev. Lett. **67**, 2784 (1991).
[16] A. Derevianko and S. G. Porsev, Phys. Rev. A **65**, 052115 (2002).
[17] S. G. Porsev, K. Beloy, and A. Derevianko, Phys. Rev. D **82**, 036008 (2010).
[18] V. A. Dzuba, J. C. Berengut, V. V. Flambaum, and B. Roberts, Phys. Rev. Lett. **109**, 203003 (2012).
[19] M. Gunawardena and D. S. Elliott, Phys. Rev. Lett. **98**, 043001 (2007).

[20] M. Gunawardena and D. S. Elliott, Phys. Rev. A **76**, 033412 (2007).
[21] S. L. Gilbert and C. E. Wieman, Phys. Rev. A **34**, 792 (1986).
[22] A. A. Vasilyev, I. M. Savukov, M. S. Safronova, and H. G. Berry, Phys. Rev. A **66**, 020101 (2002).
[23] D. Cho, C. S. Wood, S. C. Bennett, J. L. Roberts, and C. E. Wieman, Phys. Rev. A **55**, 1007 (1997).
[24] S. C. Bennett and C. E. Wieman, Phys. Rev. Lett. **82**, 2484 (1999).
[25] V. A. Dzuba, V. V. Flambaum, and J. S. M. Ginges, Phys. Rev. D **66**, 076013 (2002).
[26] J. S. M. Ginges and V. V. Flambaum, Phys. Rep. **397**, 63 (2004).
[27] V. V. Flambaum, I. B. Khriplovich, and O. P. Sushkov, Phys. Lett. A **67**, 177 (1978).
[28] I. M. Savukov, A. Derevianko, H. G. Berry, and W. R. Johnson, Phys. Rev. Lett. **83**, 2914 (1999).
[29] B. Cagnac, G. Grynberg, and F. Biraben, J. Phys. (Paris) **34**, 345 (1973).
[30] G. Grynberg and B. Cagnac, Rep. Prog. Phys. **40**, 791 (1977).
[31] K. D. Bonin and T. J. McIlrath, J. Opt. Soc. Am. B **1**, 52 (1984).
[32] V. Gerginov and C. E. Tanner, Opt. Commun. **222**, 17 (2003).
[33] C. S. Wood, Ph.D. thesis, University of Colorado, 1996.
[34] S. L. Gilbert, R. N. Watts, and C. E. Wieman, Phys. Rev. A **29**, 137 (1984).
[35] M. A. Bouchiat, J. Guéna, and L. Pottier, J. Phys. Lett. **45**, L61 (1984).
[36] S. C. Bennett, Ph.D. thesis, University of Colorado, 1998.
[37] S. Saraf, R. L. Byer, and P. J. King, Appl. Opt. **46**, 3850 (2007).